# A Discrete State Event Driven Simulation based Losses Analysis for Multi-terminal Megawatt Power Electronic Transformer

Jialin Zheng, *Student Member*, *IEEE*, Zhengming Zhao, *Fellow*, *IEEE*, Bochen Shi, *Student Member*, *IEEE*, Zhujun Yu, *Student Member*, *IEEE*, Jiahe Ju, *Student Member*, *IEEE*, and Zhiqiang Fan

***Abstract*—At present, power electronic transformers (PETs) have been widely used in power systems. With the increase of PET capacity to the megawatt level. the problem of increased losses need to be taken seriously. As an important indicator of power electronic device designing, losses have always been the focus of attention. At present, the losses are generally measured through experiments, but it takes a lot of time and is difficult to quantitatively analyze the internal distribution of PET losses. To solve the above problems, this article first qualitatively analyzes the losses of power electronic devices and proposes a loss calculation method based on pure simulation. This method uses the Discrete State Event Driven (DSED) modeling method to solve the problem of slow simulation speed of large-capacity power electronic devices and uses a loss calculation method that considers the operating conditions of the device to improve the calculation accuracy. For the PET prototype in this article, a losses model of the PET is established. The comparison of experimental and simulation results verifies the feasibility of the losses model. Then the losses composition of PET was analyzed to provide reference opinions for actual operation. It can help pre-analyze the losses distribution of PET, thereby providing a potential method for improving system efficiency.**

***Index Terms*—Power electronic transformer (PET), losses analysis, efficiency, losses branch model, discrete-state event-driven.**

## I. Introduction

In recent years, power electronic transformer (PET) has been widely used in smart grid, AC/DC hybrid power grid, and locomotive traction system, which has attracted the attention of industry and academia. At present, researchers mainly focus on the topology of PET [1]-[3], high-frequency transformer design [4]-[6], and control strategy [7]-[8]. However, there are still some problems needed to be solved, such as the cluster control, the oscillation of high-frequency bus, and the losses analysis problem [9]. Losses analysis is very worthy of study because a detailed losses analysis can methodically interpret the energy consumption, and then help researchers propose methods to reduce the losses.

At present, the method of measuring the efficiency curve of the device is as follows. First, several sets of losses curves under different working conditions are measured through experiments, and then the efficiency curve of the entire device can be obtained by fitting these curves [10]-[12]. Although the principle of this method is simple, it takes a lot of time to do experiments for large-capacity power electronic equipment. Moreover, this method cannot accurately obtain the losses under each operating condition [13]. In order to quickly and accurately obtain the losses under various working conditions, computer simulation methods can be used. Detailed physical models of equipment are now commonly used to calculate losses [14]-[15]. Because the calculation results of the detailed physical model are basically consistent with the experimental results. This method is feasible for small-scale power electronic circuits. However, for large-scale power electronic circuits, the calculation time for detailed physical model may be as long as several hours, which is often unacceptable. Therefore, scholars use the ideal switch model to solve large-scale power electronic circuits, and then use the datasheet to calculate the losses [16]-[17]. We know that the losses in the datasheet is measured through a double pulse experiment, this oprating condition is quite different from the actual device operating conditions. The error calculated by this method is relatively large. In summary, for large-capacity power electronic circuits, there is still a lack of accurate loss calculation methods.

This article proposes a loss calculation method for large-capacity power electronic devices and a loss calculation model for the PET studied in this article. The model calculates the losses of PET by using the voltage and current value in each component of the PET under different working conditions. It is hard to calculate these values in general simulation, because the megawatt PET usually contains a large amount of power electronic equipment. Traditional simulation software uses a time-driven approach, which consumes a lot of time in the calculation of the positioning switch timing. This paper uses a discrete state event-driven simulation (DSED) platform [18] to calculate the voltage and current. Using the DSED simulation platform can improve the accuracy of the simulation and quickly simulate multiple sets of working conditions for a long

Manuscript received September 01, 2020; revised October 20, 2020; accepted November 18, 2020.date of publication December 25, 2020; date of current version December 18, 2020.

This work was supported by the National Key Research and Development Program of China (2017YFB0903200). *(Corresponding author: Zhengming Zhao*)

The authors are with the Department of Electrical Engineering, Tsinghua University, Beijing 100084, China (e-mail:zhengjl19@mails.tsinghua.edu.cn; zhaozm@tsinghua.edu.cn; shbch03@126.com;yuzhujun14@hotmail.com; jujh18@mails.tsinghua.edu.cn; fanzq19@mails.tsinghua.edu.cn)

Digital Object Identifier 10.30941/CESTEMS.2020.00034

time. The voltage and current are calculated by DSED simulation platform. Using these parameters, the losses can be calculated by the losses model without repeated experiments.

The structure of this paper is as follows: Section II introduces the topology and principle of the PET studied in this article and give a basic losses analysis of power electronic devices; Section III introduces the DSED simulation principle and obtains the losses model using the losses expression considering the working condition of each module; Section IV verifies the accuracy of the losses model through the actual experiment and three applications are proposed to reflect the advantages of the loss model; Finally, the conclusions are summarized in Section V.

## II. Topology, Principle and Losses Analysis of PET

### A. Topology and Principle

Power electronic transformers have a variety of topologies. Common topologies mostly use common DC bus topologies, which can be divided into two types: cascaded H-bridge structure [19] and modular multi-level structure [20]. A cascaded H-bridge structure 10 kV-2 MW 4-port PET is investigated in this paper. Its structure adopts modular multi-active bridge (MMAB) the papers [21]-[22] proposed. The main circuit is shown in Fig 1. The topology uses 'H-bridge unit + high-frequency transformer' as a power module, and each module is connected to the high-frequency AC bus through high frequency transformer (HFT). The AC side (HFT side) of these sub-modules are connected in parallel through a common low-voltage high-frequency bus, and the DC side can be expanded into ports of any voltage/power level by using a series/parallel combination. In addition, it can expand any number of ports and ensure that the ports are isolated from each other based on the common low-voltage high-frequency bus.

The PET examined in this paper has 4 ports: HVAC port is used as input and connected to 10 kV AC grid; HVDC port, LVDC port and LVAC port output 10 kV DC, ±375 V DC and 380 V AC respectively. It can realize the flexible access and energy routing of multiple distributed energy and loads. The whole device contains 87 sub-modules, 72 high-frequency transformers and 578 switching devices, the scale is very large; and the highest switching frequency is 20kHz. The rated power of the four ports is 1 MW, and the simulation example structure is shown in Fig 1.

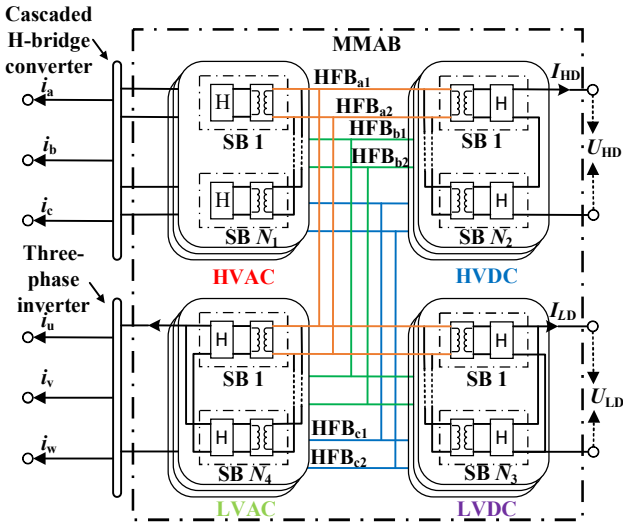


Fig. 1. The topology of PET

### B. Basic Losses analysis

Losses is an important indicator of power electronic devices. The losses simulation can provide an important reference for device design. It is necessary to find out the losses composition of power electronic devices

The converter input power $P_{in}$ is equal to the sum of output power $P_{out}$ and power loss $P_{loss}$. The power loss mainly includes device on-state loss $P_{on}$, device switching loss $P_{sw}$, transformer copper loss $P_{Cu}$, transformer iron loss $P_{Fe}$, capacitor and inductor equivalent resistance loss $P_{ESR}$, and additional loss $P_0$. All the above loss calculation formulas can be seen in Appendix I.

$$\begin{cases} P_{in} = P_{out} + P_{loss} \\ P_{loss} = P_{on} + P_{sw} + P_{Cu} + P_{Fe} + P_{ESR} + P_0 \end{cases} \tag{1}$$

The output voltage of PET is fixed. As the load changes, the output current of the device also changes. Therefore, it is necessary to make clear the relationship between these different losses and the load current It can be seen that, according to the relationship with the load current $I_L$, the losses in the converter can be divided into three mechanisms, fixed loss $P_{fixed}$, switching loss $P_{sw}$ and resistive loss $P_R$. The fixed loss $P_{fixed}$ does not change with the load current. , The switching loss $P_{sw}$ is approximately proportional to the first order of the load current, and the resistive loss $P_R$ is approximately proportional to the second order of the load current. The main components of fixed loss and resistive loss are

$$\begin{cases} P_{fixed} = (P_{Fe} + P_0) \propto I_L^0 = 1 \\ P_{sw} \propto I_L^1 = I_L \\ P_R = (P_{on} + P_{Cu} + P_{ESR}) \propto I_L^2 \end{cases} \tag{2}$$

Therefore, the device efficiency will change with the load current under the losses of these three different mechanisms. The function of the efficiency curve is expressed as

$$\eta(I_L) = 1 / \left( 1 + \frac{A + BI_L + CI_L^2}{I_L} \right) \tag{3}$$

Among them, A, B, C are coefficients, which represent fixed losses, switching losses and resistive losses respectively. Taking the derivative of equation (3), and we can find the position of the maximum efficiency point.

$$I_L(\eta_{\max}) = I_L \mid_{d\eta / dI_L = 0} = \sqrt{A / C} \tag{4}$$

Thus, the shape of the efficiency curve of a typical power electronic converter can be estimated, as shown in Fig 2. The low efficiency at light load is mainly due to the fact that the fixed loss $P_{fixed}$ accounts for a larger proportion of the load; the low efficiency at heavy load is mainly because the resistive loss $P_R$ increases twice with the load, resulting in a decrease in efficiency. The load corresponding to the maximum efficiency

point of the device depends on the relative relationship between these two losses, or the relationship between the coefficients A and C in equation (5). According to experience, the maximum efficiency point of power electronic devices is usually between 50% and 80% of the maximum load.

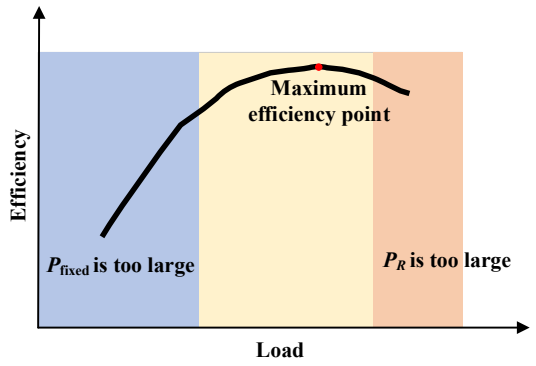


Fig. 2. Efficiency curve of a typical power electronic device

## III. PET Losses Model Based on DSED Simulation Method

In the previous section, the basic analysis of PET losses has been carried out, and the calculation of losses through simulation has become a problem to be solved. To achieve this goal, we need to calculate the losses of each part according to the composition of PET. After getting the losses expression, we also need to calculate the parameters of the losses model through simulation. However, the simulation speed of large-scale power electronics has always been slow. In this paper, DSED method is used to solve the simulation problem of PET, and the simulation results are brought into the losses model to quickly obtain the losses and efficiency of PET under different working conditions.

The following will first introduce DSED method, and then give the losses expression for calculation. Finally, the losses expression of pet is given by combining the two parts.

### *A. DSED Algorithm*

At present, most power electronics simulation software such as PSIM®, Simulink®, PLECS®, etc. do not have the ability to consider the switching transient process in detail, while Saber®, PSpice® and other software have switching device transient models[18], However, it cannot be used in actual device simulation, especially large-capacity power electronic system simulation, for three reasons: unacceptable simulation speed, frequent convergence problems[23] and experimental parameter extraction methods [24-25].

These simulation tools are more practical in simple circuit simulation composed of several switching devices, but large-capacity power electronic devices are often composed of hundreds or even thousands of switching devices, and The price is unacceptable using Saber® and other software for transient simulation[25]. Even if using the ideal switch model for simulation, the simulation speed of existing simulation tools is also difficult to meet the needs of large-capacity power electronic devices.

For example, take the simulation example of this article as an example: a 10 kV-2 MW PET, the entire device is composed of 87 conversion unit modules, 578 switching devices, and 72 high-frequency transformers. If you use the now commercially available and mature power electronics simulation software PLECS® for simulation, the 0.5 s dynamic process will take about 10 hours if the accuracy is not set very high, while it will spend a longer time using Simulink® and other software to achieve the same accuracy. The speed is completely insufficient to meet the needs of device development.

The DSED simulation method is proposed for the two goals of transient simulation and high-efficiency simulation[12-13].] The method innovated in many aspects such as transient models, numerical algorithms, simulation mechanisms, and modules decoupling combining the mathematical characteristics of power electronic systems. the simulation speed of power electronic circuits has been greatly improved. The details of the DSED algorithm can be found in the literature[12-13].

### *B. Comparison of simulation results between DSED and PLECS®*

In order to verify the accuracy of DSED, simulation examples of 4-port PET were built for comparison by using DSED simulation method and the current mature power electronics simulation software PLECS®. Among them, PLECS® uses version 4.1.8. The test scenarios are starting process and switching load. Each bus capacitor of the device is pre-charged to the rated value, starting with 500 kW of LVAC load, and putting into HVDC load of 250 kW at 0.1 s.

The port waveforms are shown in Fig 3, which (a) is HVAC grid-side current, (b) is HVDC output voltage, and (c) is LVAC output voltage. The comparison of the calculation points of the two simulation software can be seen in the partial magnified figure (d).

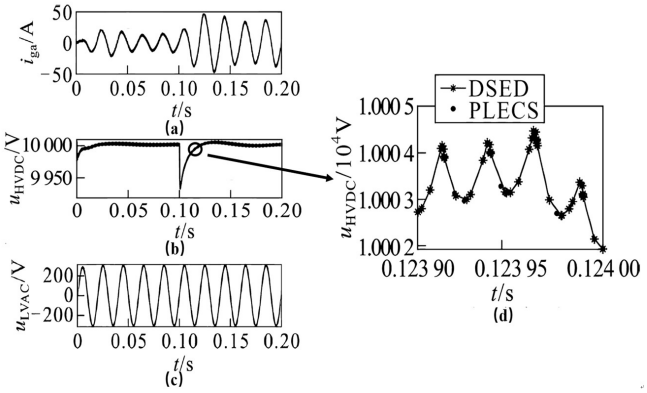


Fig. 3. Comparisons of simulated results

From the above comparison results, it can be seen that the simulation results of DSED and PLECS® are basically the same regardless of the port output characteristics or the internal characteristics of the device. Table I shows the comparison of the time-consuming simulation and the error comparison of the simulation results. The error calculation is based on the results obtained by the PLECS® simulation software and limiting the maximum step size to 10e−8. The accuracy of the simulation results obtained below is sufficiently high.

TABLE I
EFFICIENCY COMPARISONS BETWEEN DSED AND PLECS®

| | | DSED | PLECS® |
|---|---|---|---|
| Simulation process | | 0.2 s dynamic process | 0.2 s dynamic process |
| Simulation Sets | | Variable step algorithm Maximum step size 10e−3 Minimum/maximum order 2/10 Absolute error 10e-3 | Variable step algorithm RADAU solver Maximum step size 10e−3 Absolute error 10e−4 |
| Switching Model | | Ideal Model | Ideal Model |
| Time Cost | | 14.6s | 6h 32min |
| Relative error | Grid current | 0.001 53% | 0.002 32% |
| | HVDC port voltage | 0.000 0431% | 0.000 0245% |
| | LVDC port current | 0.017 3% | 0.026 2% |

Note:
$\text{error1} = |DSED - PLECS| / DSED, \text{error2} = |DSED - PLECS| / PLECS$

### C. Losses Model

The PET is composed of switching devices, high-frequency transformers, passive devices, and control circuits. The losses of the control circuit and passive devices account for a small proportion and can be ignored [26]. The losses are mainly caused by switching devices and high-frequency transformers.

Both Insulated Gate Bipolar Transistor (IGBT) and silicon carbide Metal-Oxide-Semiconductor Field-Effect Transistor (SiC MOSFET) [27] are used in the PET we investigate. Two switching devices are used in different parts of the PET according to their advantage. The losses analysis for both of them will be given in Appendix I.

After deriving the losses expression of each switching device, it is necessary to consider the above losses in the actual converter.

a) The Conduction Losses of Converters

The conduction losses in the switching device can be calculated based on Eq (21), (22), (23). The IGBT on-state losses can be expressed as,

$$P_{IGBT,on} = \frac{1}{T}\int_0^T (u_{CE} \times i_C) d\varpi t = U_{CE0} I_{IGBT,av} + R_T I_{IGBT,rms}^2 \quad (5)$$

where $I_{\text{IGBT,av}}$ is the average current of IGBT, and $I_{\text{IGBT,rms}}$ is the RMS current of IGBT.

Similarly, the MOSFET and diode on-state losses can be expressed as,

$$P_{MOSFET,on} = \frac{1}{T}\int_0^T (u_{DS} \times i_D) d\varpi t = R_T I_{MOSFET,rms}^2 \quad (6)$$

$$P_{diode,on} = \frac{1}{T}\int_0^T (u_D \times i_D) d\varpi t = U_{D0} I_{diode,av} + R_D I_{diode,rms}^2 \quad (7)$$

where $I_{\text{MOSFET,rms}}$ is the RMS current of SiC MOSFET, where $I_{\text{diode,av}}$ is the average current of diode, and $I_{\text{diode,rms}}$ is the RMS current of diode.

b) The Switching Losses of Converters

The turn-on losses $E_{\text{on}}$ and turn-off losses $E_{\text{off}}$ are calculated in Eq (24) and (25). Then, the average switching losses of IGBT can be calculated as follow,

$$\begin{aligned} P_{IGBT,switch} &= \frac{1}{T}\sum_{j=1}^{N}\left(E_{on}(i(j)) + E_{off}(i(j))\right)\frac{i(j)}{I_{rate}} \bullet \frac{U_{dc}}{U_{rate}} \\ &= \frac{1}{T}\sum_{j=1}^{N}\left((k_1+k_3)i(j)+k_2\right)\frac{i(j)}{I_{rate}} \bullet \frac{U_{dc}}{U_{rate}} \end{aligned} \quad (8)$$

where $N$ is the switching times in half grid cycle， $I_{\text{rate}}$ and $U_{\text{rate}}$ are the rated values of current and voltage during the switching losses test in device datasheet, *i(j)* and $U_{\text{dc}}$ are the real values of IGBT current and voltage in the PET.

Similarly, the switching losses of MOSFET and diode can be expressed as,

$$P_{Mosfet,switch} = \frac{1}{T}\sum_{j=1}^{N}\left((k_6+k_8)i(j)+k_7+k_9\right)\frac{i(j)}{I_{rate}} \bullet \frac{U_{real}}{U_{rate}} \quad (9)$$

$$P_{diode,switch} = \frac{1}{T}\sum_{j=1}^{N}\left(k_4 i(j)+k_5\right)\frac{i(j)}{I_{rate}} \bullet \frac{U_{real}}{U_{rate}} \quad (10)$$

### D. Losses Model of PET based on DSED

After deriving all the components losses expression of PET and calculating the current and voltage needed by losses expression using DSED method, the losses of each module in the PET can be analyzed.

According to the above analysis, the losses can be divided into three types: they are directly proportional to $I^n$ (n = 0, 1, 2).

$$P_{loss} = a \times i^2 + b \times i + c \quad (11)$$

a) High Voltage AC Module

By using Eq (5)-(10), the losses of each part in high voltage AC module is calculated using DSED simulation,

$$P_{hvac,vsc} = a_1 I_{ac}^2 + b_1 I_{ac} + c_1 \quad (12)$$

$$P_{hvac,dab} = a_2 I_{dab}^2 + b_2 I_{dab} + c_2 \quad (13)$$

$$P_{hvac,HFT} = P_{Cu} + P_{Fe} \quad (14)$$

where $P_{\text{hvac,vsc}}$ is the losses of AC-DC H-bridge, $P_{\text{hvac,dab}}$ is the losses of DAB H-bridge, $P_{\text{hvac,HFT}}$ is the losses of HFT, $a_1$, $a_2$, $b_1$, $b_2$, $c_1$, $c_2$ are constants.

b) Low Voltage AC Module

The low voltage AC module is composed of a DAB H bridge and an AC-DC H bridge. By using Eq (5)-(10), the losses of each part are calculated as,

$$P_{lvac,vsc} = a_3 I_{ac}^2 + b_3 I_{ac} + c_3 \quad (15)$$

$$P_{lvac,dab} = a_4 I_{dab}^2 + b_4 I_{dab} + c_4 \quad (16)$$

where $P_{\text{lvac,vsc}}$ is the losses of AC-DC H-bridge, $P_{\text{lvac,dab}}$ is the losses of DAB H-bridge, $a_3$, $a_4$, $b_3$, $b_4$, $c_3$, $c_4$ are constants.

c) High and Low Voltage DC module

The module structure of the two DC ports is the same, which can be analyzed together. The DC module consists of an H bridge using SiC MOSFET and an HFT shown in Fig 1.

By using Eq (5)-(10), the losses of each part in high voltage AC module is calculated as,

$$\begin{aligned} P_{hvdc,dab} &= a_5 I_{dab}^2 + b_5 I_{dab} + c_5 \\ P_{lvdc,dab} &= a_6 I_{dab}^2 + b_6 I_{dab} + c_6 \\ P_{hvdc,HF} &= P_{Cu2} + P_{Fe2} \\ P_{lvdc,HF} &= P_{Cu3} + P_{Fe3} \end{aligned} \tag{17}$$

where $P_{\text{hvdc,dab}}$, $P_{\text{lvdc,dab}}$ are the losses of H-bridge in high voltage DC module's DAB and low voltage DC module's DAB, $P_{\text{hvdc,HFT}}$, $P_{\text{lvdc,HFT}}$ is the losses of HFT in high voltage DC module and low voltage DC module, $a_5$, $a_6$, $b_5$, $b_6$, $c_5$, $c_6$ are constants.

All the constant coefficients $a_i$, $b_i$, $c_i$($i$=1, 2, 3, 4, 5, 6) can be calculated by using losses expression we get before and DSED simulation method.

The voltage of each part of the device is unchanged. By changing the current in the expression into power, the losses expression can be easily normalized with different parameters $a^*$, $b^*$, $c^*$ as,

$$P_{loss} = a^* \times P^2 + b^* \times P + c^* \tag{18}$$

The losses in each part of PET can be shown in Fig 4. Considering the number of submodules in each port, the losses of each port can be calculated by using Eq (5)-(19). The constant coefficients of each port can be driven and the following expression is the PET losses under a certain condition that AC loop power is 500 kW, and DC loop power is 400 kW.

$$\begin{aligned} P_{loss,hvac} &= 0.49\text{e-}5 \times P_{hvac}^2 + 29.249\text{e-}4 \times P_{hvac} + 6.5418 \\ P_{loss,hvdc} &= 0.509\text{e-}5 \times P_{hvdc}^2 + 6.512\text{e-}4 \times P_{hvdc} + 3.9635 \\ P_{loss,lvdc} &= 0.983\text{e-}5 \times P_{lvdc}^2 + 25.08\text{e-}4 \times P_{lvdc} + 3.649 \\ P_{loss,lvac} &= 0.503\text{e-}5 \times P_{lvac}^2 + 4.6794\text{e-}4 \times P_{lvac} + 3.5975 \end{aligned} \tag{19}$$

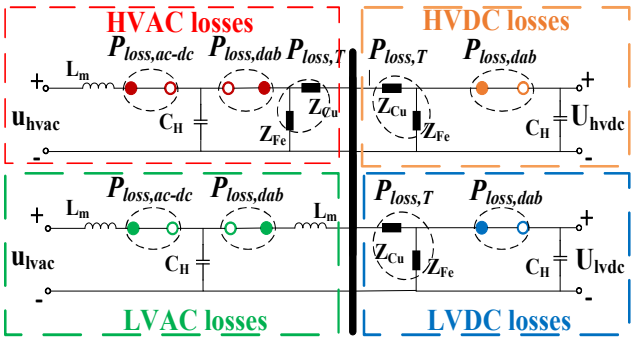


Fig. 4. The losses model of PET

## IV. Validation and Application of Losses Model

The validation of the losses model is proved through experiments and then the advantages of using the losses model are illustrated through three examples.

### A. The Validation of the Losses Model

A 1MW PET prototype is used for case study to verify the correctness of the model. The prototype is shown in Fig 5.

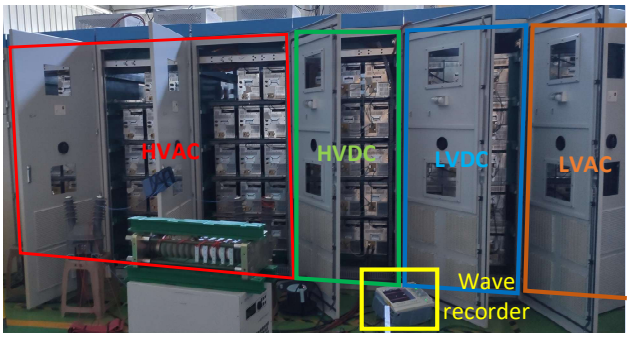


Fig. 5. Experimental test platform

The 1MW PET adopts the DAB module shown in Fig 1 and has four voltage level ports. The high voltage AC port rated capacity is 1MW, the high voltage DC port rated capacity is 500kW, the low voltage DC port rated capacity is 1MW, the low voltage AC port rated capacity is 700kW, the modulation index of AC-DC H-bridge is 1, and the frequency of HFT is 20kHz. The MOSFET modules use CREE' CAS120M12BM2 and CAS300M12BM2 and the IGBT modules use Infineon's FF1400R12IP4. The high voltage AC port consists of 14 input series output parallel (ISOP) modules in each phase. The high voltage DC port and the low voltage DC port have 15 modules paralleled respectively. The low voltage AC port has 15 DAB modules and a 3 phase 4 legs inverter composed of IGBT. Each port can be used as a source to transmit power or as a load to absorb power.

The experimental working condition is shown in Fig 6. Two DC ports are connected to form a power closed loop. One of them is in power control mode and the other is in voltage control mode. Power can flow from one DC port to another. The high voltage AC port is connected to the grid and operates in the following mode. The low-voltage AC port runs in the control power mode, and the power flows back to the grid through the transformer.

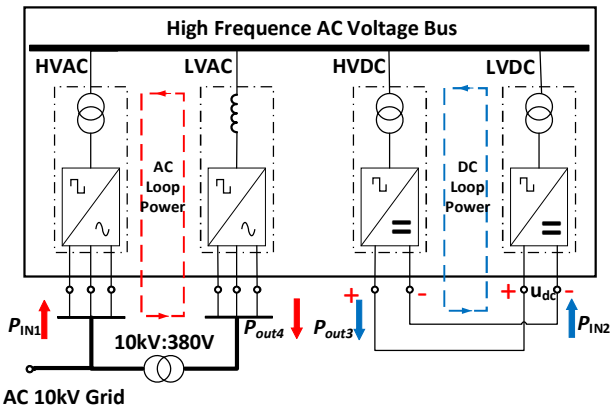


Fig. 6. The experimental topology of PET losses test

In the experiment, the power reference value of AC loop and DC loop are changed respectively. The DC loop increases by 100kW from 0kw to 500kW, and the AC loop increases by 100kW from 0kw to 400kW. The total input power and output power were experimentally recorded, and the losses of PET were obtained, as shown in Table II.

As for the simulation, the voltage and current required for losses calculation are calculated by DSED method to improve

TABLE II
LOSSES FROM EXPERIMENT AND SIMULATION

| AC Loop Power(kW) | DC Loop Power(kW) | Experiment Result(kW) | Simulation Result(kW) | error |
|---|---|---|---|---|
| 100 | 0 | 20.2 | 18.41 | 8.86% |
| 100 | 100 | 19.2 | 18.68 | 2.71% |
| 100 | 200 | 20.2 | 19.25 | 4.70% |
| 100 | 300 | 21.2 | 20.13 | 5.05% |
| 100 | 400 | 22.2 | 21.32 | 3.96% |
| 100 | 500 | 23.2 | 22.81 | 1.68% |
| 200 | 0 | 20.2 | 19.40 | 3.96% |
| 200 | 100 | 20.2 | 19.66 | 2.67% |
| 200 | 200 | 21.2 | 20.23 | 4.58% |
| 200 | 300 | 21.2 | 21.11 | 0.42% |
| 200 | 400 | 22.2 | 22.30 | 0.45% |
| 200 | 500 | 24.2 | 23.80 | 1.65% |
| 300 | 0 | 21.2 | 20.68 | 2.45% |
| 300 | 100 | 20.2 | 20.94 | 3.66% |
| 300 | 200 | 21.2 | 21.51 | 1.46% |
| 300 | 300 | 22.2 | 22.39 | 0.86% |
| 300 | 400 | 22.2 | 23.58 | 6.22% |
| 300 | 500 | 24.2 | 25.08 | 3.64% |
| 400 | 0 | 21.2 | 22.25 | 4.95% |
| 400 | 100 | 22.2 | 22.52 | 1.44% |
| 400 | 200 | 21.2 | 23.09 | 8.92% |
| 400 | 300 | 22.2 | 23.97 | 7.97% |
| 400 | 400 | 25.2 | 25.16 | 0.16% |
| 400 | 500 | 26.2 | 26.65 | 1.72% |

Note: error = $|Experiment - Simulation| / Experiment$

the accuracy and speed of simulation [28]. By utilizing the losses branch model of PET and simulating the actual operation of a PET, the losses obtained from the simulation is shown in Table I.

It is found that the average error between the experimental value and the simulation value is 3.51% from Table I. The maximum error is 8.92% when the AC loop is 400kW and the DC loop is 200kW. At this point, the absolute error between the experimental value and the theoretical value is 1.89kW at the maximum.

The main reasons for the difference between the simulated value and the experimental value are as follows:

This article is concerned with providing a method for quickly calculating the loss and efficiency of large-scale power electronic devices. The thermal calculation inside the device is not the focus of this article. In the experiment, the device temperature is room temperature when the device starts to run. The temperature of the device will rise as the experiment progresses. According to the interaction of heat and heat dissipation of the device, the temperature of the device will remain basically unchanged in the end. This article calculates the switching loss using the loss value of 125 °C in the device data sheet, because this temperature is close to the actual temperature. The device temperature of the actual device will change and this will cause errors.

In addition, only a few main losses are considered in the simulation, and the loss of the driver board, the loss of the cooling fan, and the loss of the inductor and capacitor are not considered. In addition, When measuring the efficiency there is a number of things to consider, including the accuracy of the power meter used in the experimental measurement and so on. All of the above will cause errors in the results. Although the relative error between the simulated value and the experimental value is large, the absolute error is small. It has little effect on

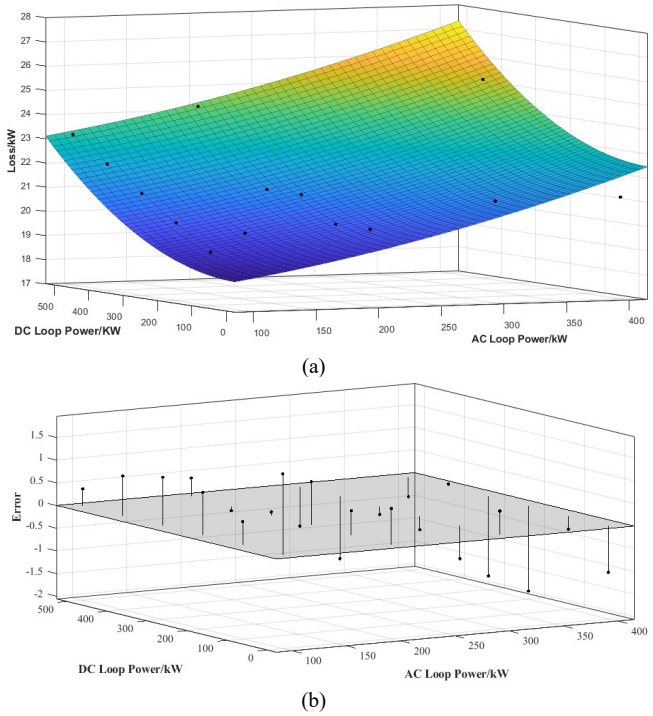

Fig. 7. Fitting degree(a) and Error(b) between Simulation and Experiment

the efficiency curve and loss distribution of the research device.

From Fig 7 (a), we can see that the losses surface calculated by the losses model is consistent with the measured losses data. The R-square of the simulation losses curve is 0.7012. The error between simulation value and experimental value is shown in Fig. 7 (b), and the maximum error is 1.89 kW, the minimum error is 0.05 kW.

Through the above analysis, the accuracy of the proposed losses branch model can be verified.

### *B. The Application of Losses Model*

After verifying the accuracy of the loss model, we believe that the proposed model is basically consistent with the experimental results. Therefore, we can use this model to implement functions that were difficult to achieve before. For example, find the maximum efficiency point, the losses distribution of the device, and the relationship of various losses with load. These are usually difficult to obtain through experiments, but they are very useful for our research and design of devices. The details will be expanded below.

a) Search for The Maximum Efficiency Point

It is known that the device operating near the maximum efficiency point has the greatest economic benefit, especially for the megawatt power electronic transformer discussed in this paper. For this kind of large device, because the simulation speed is too slow, we can only use the experiment to find the maximum efficiency point. However, the disadvantage of finding the maximum efficiency point through experiments is that the search step size is very large, which often cannot accurately find the real maximum efficiency point. Moreover, this large-scale equipment needs a lot of time to do the

experiment, including the inspection before the start, the pre charging of the device and so on. The above problems can be solved by using the loss calculation method proposed in this paper.

Taking one working condition as an example, the two DC ports power of PET can be changed and the AC ports power is determined. The efficiency curve can be obtained through the losses model, as shown in Fig 8. When the DC power of the PET is 325 kW, the maximum efficiency of the PET is 98.14%.

The maximum efficiency point of the device is obtained by this method. The simulation time is much less than the actual experiment, and the search step is quite small to accurately find the maximum efficiency point. This method provides suggestions for the actual operating conditions of the device, makes the device run as close as possible to the maximum efficiency point, and improves the efficiency of the device operation.

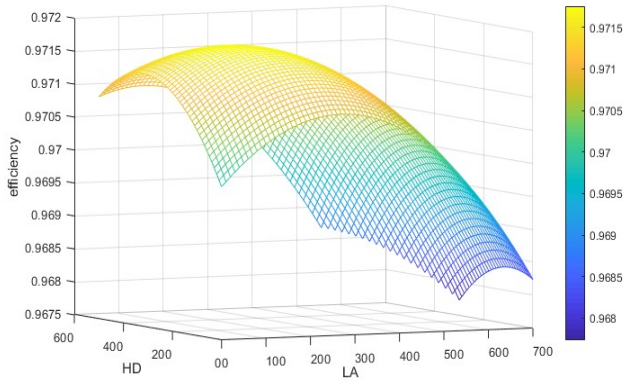


Fig. 8. The efficiency curve of four-ports PET

b) The Losses Distribution Analysis

It is quite meaningful to study the loss distribution inside the device. Generally, we can only get the total loss of PET of the device through experiments, and it is difficult to know the loss of each part of the device. As far as the PET studied in this article is concerned, it has four ports, and each port has different losses due to different operating conditions. The loss of each port needs to be obtained by multiple sets of experiments, which takes a lot of time, but only the loss of each port can be known. The method proposed in this paper, due to the use of event-driven simulation algorithms, can simulate large-scale power electronic devices extremely quickly. Therefore, not only the loss of each port and the loss of the entire device can be obtained, but also the loss caused by the switching devices and transformers in each device can be known. In this way, it is convenient to find the losses with the largest proportion of losses under different working conditions, so that priority can be given to the larger losses to optimize and reduce losses.

The losses distribution of the PET can be seen from Fig 9. The winding losses and additional losses are unchanged during load changes. The relationship between switching losses and load is linear and the relationship between core losses and load is quadratic. Therefore, the PET losses can be reduced according to the distribution of losses and the load size of the PET operation. If the PET needs to be operated under heavy load for a long time, reducing HFT winding losses is the first consideration. If the PET is under light load for a long time, reducing HFT core losses is the first consideration.

c) The Relationship of Losses with Load.

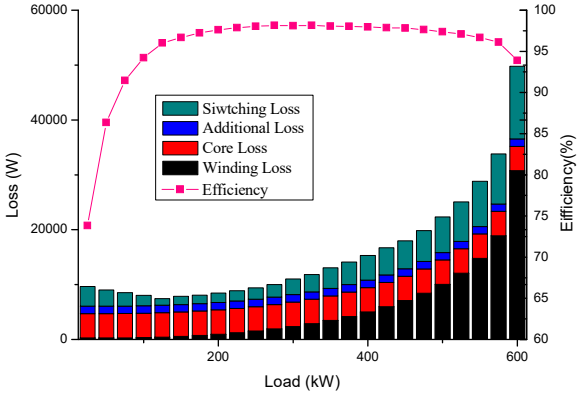


Fig. 9. The efficiency and losses distribution of two DC ports

The method proposed in this article can study the relationship between each type of loss and load. The curves of absolute value and relative value of each kind of losses with load are shown in Fig 10, respectively. It can be seen that the absolute value of fixed losses such as losses and additional losses remains unchanged, and its relative value decreases with the increment of load, so the efficiency shows an increasing trend; the switching losses present a quadratic relationship with the load power, which has little effect on the position of the maximum efficiency point; while the resistive losses increases in a quadratic way, and its relative load power proportion is increasing. The efficiency curve decreases under heavy load. Under light load, the main losses are transformer iron losses, accounting for more than 50%; under full load, the main losses are switching losses, and the proportion of resistive losses has been greatly increased. The PET can be optimized according to the relation of losses and load obtained by the losses model.

In general, the loss calculation method proposed in this

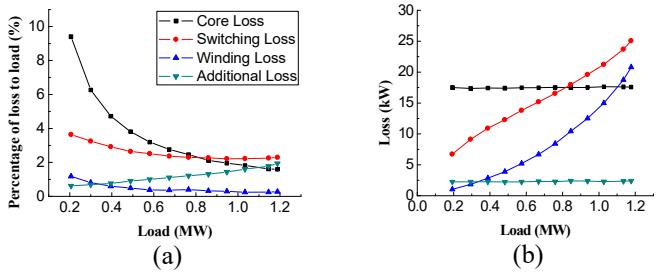


Fig. 10. The losses distribution of four-port PET

article can not only calculate the loss of each element inside the device, but also calculate the loss of the entire device. Compared with the previous method, the method proposed in this paper can greatly improve the simulation speed while the simulation results are basically the same as the experimental results.

## V. Conclusion

This article mainly solves the problem of not being able to quickly and accurately simulate the loss of high-power power electronic equipment. The main contributions of this article are as follows:

1. This article conducts a general analysis of the efficiency of power electronic equipment, and sorts out the loss calculation methods of switching equipment and transformers contained in power electronic equipment.
2. The calculation of equipment loss needs to know the voltage and current of each switchgear and transformer in the equipment, and all current commercial software (such as PET) used for high-power power electronic equipment has the problem of slow simulation speed, so this article innovatively The new method using DSED can greatly improve the simulation speed of the device. This method can simulate the cluster operation scenario of multiple large-capacity devices, thereby providing strong support for the research of electronic power system (eGrid).
3. This paper proposes a loss analysis model combined with the DSED algorithm, which is basically consistent with the experimental results. This loss model can calculate the loss from the switching device to each port to the entire device, and solves the problem that it is difficult to know the loss of each component inside the device and find the main loss for optimization when actually measuring the loss. This loss analysis and calculation method has the characteristics of high accuracy and fast speed, due to the innovative use of DSED algorithm and loss calculation based on topology and control algorithm. This method can provide support for the design and loss analysis of large-capacity power electronic devices and provide a set of powerful analysis tools.

## Appendix I
## Basic Component Losses Expression

The power losses of power electronic devices mainly include four parts: on-state losses $P_{on}$, turn-on losses $P_{turn\text{-}on}$, turn-off losses $P_{turn\text{-}off}$ and off-state losses $P_{off}$. The off-state losses $P_{off}$ can be ignored since it accounts for a small proportion of the total losses.

The losses of the high-frequency transformer (HFT) are another important part of the total losses. The HFT losses include core losses $P_{Fe}$ and winding losses $P_{Cu}$. The following will analyze and calculate each kind of losses.

### A. On-State Losses of IGBT / SiC MOSFET

When the switching device is in the on-state, the output characteristics of SiC MOSFET and IGBT are different [29].

The output characteristic of IGBT is shown in Fig. 11 (a), the relation between collector-emitter saturation voltage $u_{CE}$ and collector current $i_C$ can be expressed as,

$$u_{CE} = U_{CE0} + R_T \times i_C \tag{20}$$

where $U_{CE0}$ presents no-load voltage, $R_T$ is the on-state resistance of IGBT. These two parameters can be extracted from the given output characteristic curve from device datasheet.

The losses of the diode in parallel with the switching device should also be considered. When a diode is in on-state, the relation between the voltage across it ($U_D$)and the current through it ($i_D$) can be expressed as,

$$U_D = U_{D0} + R_D \times i_D \tag{21}$$

where $U_{D0}$ presents the no-load voltage, $R_D$ is the on-state resistance of the diode. We can use the same method (curve fitting) to get their value as we use in IGBT.

The output characteristic of SiC MOSFET is different from that of IGBT. The output expression of MOSFET needs to be considered separately. The expression of SiC MOSFET output characteristic (device voltage $u_{ds}$ versus device current $i_{DS}$) can be written as,

$$u_{DS} = R_M \times i_{DS} \tag{22}$$

where $R_M$ represents the on-state resistance of MOSFET.

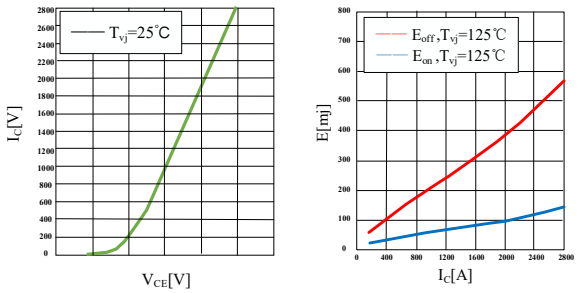


(a) (b)

Fig. 11. IGBT output characteristic curve and switching losses curve

### B. Switching Losses of IGBT / SiC MOSFET

When the switching device is working, the voltage and current of the device need time to change. The voltage and current waveform will have an overlapping area, which will cause switching losses. Switching losses expression can be calculated by adding the turn-on losses energy and turn-off losses energy in a cycle. Using the switching losses curve shown in Fig. 11 (b), the turn-on losses energy and turn-off losses energy of IGBT can be expressed as,

$$\begin{aligned} E_{on-IGBT} &= k_1 i_C + k_2 \\ E_{off-IGBT} &= k_3 i_C \end{aligned} \tag{23}$$

Similarly, the turn-on losses energy and turn-off losses energy of SiC MOSFET and the turn-off losses energy of diode can be expressed as,

$$\begin{aligned} E_{rec-diode} &= k_4 i_D + k_5 \\ E_{on-MOSFET} &= k_6 i_{DS} + k_7 \\ E_{off-MOSFET} &= k_8 i_{DS} + k_9 \end{aligned} \tag{24}$$

where $k_1$-$k_9$ are constant coefficients.

### C. Core Losses of HFT

The core losses of HFT mainly include hysteresis losses and eddy current losses [30]. The traditional transformer passes through sinusoidal voltage while HFT in Dual Active Bridge (DAB) passes through square wave voltage. Therefore, the core losses of HFT is different from that of traditional transformers. The modified formula needs to be used [31], which can be

founded as,

$$B_{\max} = \frac{V_{pri}}{4 f A_e N_w N_c}$$
$$p_{Fe} = FKf^{\alpha} B_{\max}^{\beta} \quad (25)$$
$$P_{Fe} = p_{Fe} \times V$$

where $V$ is the core effective volume in the HFT, $V_{\text{pri}}$ is the voltage of the primary side of HFT. $K$, $\alpha$, $\beta$ are constant fitting coefficients by the no-load experiment, $B_{\max}$ is the maximum value of magnetic induction intensity, $F$ is a modified flux factor when the voltage through the HFT is a square wave, $p_{\text{Fe}}$ is core loss density.

### D. Winding Losses of HFT

The HFT is mainly designed for DAB application, and its control mode in the studied prototype in this paper is single phase shift control.

The frequency of the switching device is 20kHz, the turn ratio of the designed HFT is 1:1, and the voltages $V_{\text{in}}$, $V_{\text{out}}$ of both sides are 700V.

The current waveform can be decomposed by Fourier transform to calculate the winding losses. Only odd harmonic component exists after Fourier decomposition because the current waveform is a nonsinusoidal wave and periodic symmetric function,

$$i(t) = \sum_{n=1}^{\infty} b_n I_{peak} \cos(n\varpi t) . \quad (26)$$

where $I_{\text{peak}}$ is the peak value of $i$(t), and the coefficient $b_{\text{n}}$ can be obtained by

$$b_n = \frac{4}{T} \int_0^{\frac{T}{2}} i(t) \cos(nwt) dt . \quad (27)$$

It mainly contains 20kHz, 60KHZ and 100kHz harmonics, the winding losses can be calculated as

$$P_{Cu} = \frac{1}{2} \sum_{n=1}^{5} (b_n I_{peak})^2 R_n . \quad (28)$$

where $R_{\text{n}}$ is the AC resistance corresponding to the nth harmonic current.

## REFERENCES


[1] J. Zhang, J. Liu, J. Yang, N. Zhao, Y. Wang and T. Q. Zheng, "A Modified DC Power Electronic Transformer Based on Series Connection of Full-Bridge Converters," *IEEE Transactions on Power Electronics*, vol. 34, no. 3, pp. 2119-2133, March 2019, doi: 10.1109/TPEL.2018.2842728.

[2] G. Zhang, J. Chen, B. Zhang, and Y. Zhang, "A critical topology review of power electronic transformers: In view of efficiency," *Chinese Journal of Electrical Engineering*, vol. 4, no. 2, pp. 90-95, June 2018, doi: 10.23919/CJEE.2018.8409354.

[3] J. Tian et al., "Individual DC Voltage Balance Control for Cascaded H-Bridge Electronic Power Transformer With Separated DC-Link Topology," *IEEE Access*, vol. 7, pp. 38558-38567, 2019, doi: 10.1109/ACCESS.2019.2905006.

[4] Z. Peng, G. Wang, X. Zhai, X. Zhang, H. Zhou, and C. Yi, "Optimum Design of High Frequency Transformer Based on Winding Spacing," 2019 22nd International Conference on Electrical Machines and Systems (ICEMS), Harbin, China, 2019, pp. 1-6, doi: 10.1109/ICEMS.2019.8922420.

[5] E. L. Barrios, A. Urtasun, A. Ursúa, L. Marroyo, and P. Sanchis, "High-Frequency Power Transformers With Foil Windings: Maximum Interleaving and Optimal Design," *IEEE Transactions on Power Electronics*, vol. 30, no. 10, pp. 5712-5723, Oct. 2015, doi: 10.1109/TPEL.2014.2368832.

[6] S. Djuric, G. Stojanovic, M. Damnjanovic, M. Radovanovic, and E. Laboure, "Design, Modeling, and Analysis of a Compact Planar Transformer," *IEEE Transactions on Magnetics*, vol. 48, no. 11, pp. 4135-4138, Nov. 2012, doi: 10.1109/TMAG.2012.2202642.

[7] B. Liu et al., "An AC–DC Hybrid Multi-Port Energy Router With Coordinated Control and Energy Management Strategies," *IEEE Access*, vol. 7, pp. 109069-109082, 2019, doi: 10.1109/ACCESS.2019.2933469.

[8] C. Tu, F. Xiao, Z. Lan, Q. Guo, and Z. Shuai, "Analysis and Control of a Novel Modular-Based Energy Router for DC Microgrid Cluster," *IEEE Journal of Emerging and Selected Topics in Power Electronics*, vol. 7, no. 1, pp. 331-342, March 2019, doi: 10.1109/JESTPE.2018.2878004.

[9] Y. Shen et al., "Steady-state model of multi-port electric energy router and power flow analysis method of AC/DC hybrid system considering control strategies," *The Journal of Engineering*, vol. 2019, no. 16, pp. 2794-2799, 3 2019, doi: 10.1049/joe.2018.8375.

[10] S. Bolte, N. Fröhleke and J. Böcker, "DC-DC converter design for power distribution systems in electric vehicles using calorimetric loss measurements," in *Proc. of 2016 18th European Conference on Power Electronics and Applications (EPE'16 ECCE Europe)*, Karlsruhe, 2016, pp. 1-7, doi: 10.1109/EPE.2016.7695644.

[11] A. K. Sadigh, V. Dargahi and K. A. Corzine, "Analytical Determination of Conduction and Switching Power Losses in Flying-Capacitor-Based Active Neutral-Point-Clamped Multilevel Converter," *IEEE Transactions on Power Electronics*, vol. 31, no. 8, pp. 5473-5494, Aug. 2016, doi: 10.1109/TPEL.2015.2498107.

[12] Y. H. Abraham, H. Wen, W. Xiao and V. Khadkikar, "Estimating power losses in Dual Active Bridge DC-DC converter," in *Proc. of 2011 2nd International Conference on Electric Power and Energy Conversion Systems (EPECS)*, Sharjah, 2011, pp. 1-5, doi: 10.1109/EPECS.2011.6126790.

[13] S. Wei, F. He, Z. Zhao, L. Yuan, T. Lu and J. Ma, "Power loss analysis and optimization of three-level T-type converter based on hybrid devices," in *Proc. of International Conference on Renewable Power Generation (RPG 2015),* Beijing, 2015, pp. 1-6, doi: 10.1049/cp.2015.0512.

[14] N. Soltau, D. Eggers, K. Hameyer and R. W. De Doncker, "Iron Losses in a Medium-Frequency Transformer Operated in a High-Power DC–DC Converter," *IEEE Transactions on Magnetics*, vol. 50, no. 2, pp. 953-956, Feb. 2014, Art no. 7023604, doi: 10.1109/TMAG.2013.2283733.

[15] Y. Sun, L. Hu, S. M. Malik, N. Chen, and T. Pu, "Unified method for optimal power flow of AC/DC system with PET based on extended branch model," *The Journal of Engineering*, vol. 2019, no. 16, pp. 1942-1946, 3 2019, doi: 10.1049/joe.2018.8707.

[16] X. Xu, N. Tai, Y. Hu, T. Liu, C. Fan and Q. Geng, "Study on Optimal Operation of Multi-Port Cascaded Power Electronic Transformer Cluster," in *Proc. of 2019 IEEE Sustainable Power and Energy Conference (iSPEC)*, Beijing, China, 2019, pp. 2318-2323, doi: 10.1109/iSPEC48194.2019.8975033.

[17] S. Wang, J. Liu, Z. Liu, T. Wu, X. Meng, and B. Liu, "A hierarchical operation strategy of parallel inverters for efficiency improvement and voltage stabilization in microgrids," in *Proc. of 2016 IEEE 2nd Annual Southern Power Electronics Conference (SPEC)*, Auckland, 2016, pp. 1-6, doi: 10.1109/SPEC.2016.7846149.

[18] SHI B C,ZHAO Z M,ZHU Y C. "Piecewise analytical transient model for power switching device commutation unit".*IEEE Transactions on Power Electronics*, vol. 34, no. 6, pp. 5720-5736, 2018.

[19] Feng Gaohui, Zhao Zhengming, Yuan Liqiang. Synthetical control technology of electric energy router based on energy balance relationship", *Transactions of China Electrotechnical Society*, vol. 32, no. 14, pp. 34-44, 2017.

[20] Li Zixin, Wang Pin, Chu Zunfang, et al. Research on medium- and high-voltage smart distribution grid oriented power electronic transformer", *Power System Technology*, vol. 37, no.9, pp. 2592-2601, 2013.

[21] Li K, Zhao Z, Yuan L, et al. Synergetic control of high-frequency-link based multi-port solid state transformer" in *Proc. of 2018 IEEE Energy Conversion Congress and Exposition (ECCE)*, Portland, OR, USA, 2018, pp. 5630-5635.

[22] Zumel P, Fernandez C, Lazaro A. "Overall analysis of a modular multi active bridge converter", in *Proc. of 2014 IEEE 15th Workshop on Control and Modeling for Power Electronics (COMPEL)*. *IEEE*, 2014, pp.

1-9.

[23] HEFNER A R, DIEBOLT D M. “An experimentally verified IGBT model implemented in the Saber circuit simulator”, *IEEE Transactions on Power Electronics*, vol. 9, no. 5, pp. 532-542, 1994.

[24] YAN S, ZHOU Z, DINAVAHI V. “Large-scale nonlinear device-level power electronic circuit simulation on massively parallel graphics processing architectures”. *IEEE Transactions on Power Electronics*, vol. 33, no. 6, pp. 4660-4678, 2018.

[25] BRYANT A T, KANG X, SANTI E, et al. “Two-step parameter extraction procedure with formal optimization for physics-based circuit simulator IGBT and pin diode models”. *IEEE Transactions on Power Electronics*, vol. 21, no. 2, pp. 295-309, 2006.

[26] SHENG K, WILLIAMS B W, FINNEY S J. A review of IGBT models”. *IEEE transactions on Power Electronics*, vol. 15, no. 6, pp. 1250-1266, 2000.

[27] R. Baranwal, G. F. Castelino, K. Iyer, K. Basu, and N. Mohan, "A Dual-Active-Bridge-Based Single-Phase AC to DC Power Electronic Transformer With Advanced Features," *IEEE Transactions on Power Electronics*, vol. 33, no. 1, pp. 313-331, Jan. 2018, doi: 10.1109/TPEL.2017.2669148.

[28] Puqi Ning, Tianshu Yuan, Yuhui Kang, Cao Han, Lei Li. “Review of Si IGBT and SiC MOSFET Based on Hybrid Switch”. *Chinese Journal of Electrical Engineering*, vol. 5, no. 3, pp. 20-29, 2019.

[29] T. Ohnuki, O. Miyashita, P. Lataire, and G. Maggetto, "Control of a three-phase PWM rectifier using estimated AC-side and DC-side voltages," *IEEE Transactions on Power Electronics*, vol. 14, no. 2, pp. 222-226, March 1999, doi: 10.1109/63.750174.

[30] I. Žiger, B. Trkulja, and Ž. Štih, "Determination of Core Losses in Open-Core Power Voltage Transformers," *IEEE Access*, vol. 6, pp. 29426-29435, 2018, doi: 10.1109/ACCESS.2018.2838446.

[31] J.Åström and T. Thiringer, "Modeling and measurements of losses components for different switching schemes in a three phase converter using CoolMOS transistors," in *Proc. of 2009 International Conference on Power Electronics and Drive Systems (PEDS),* Taipei, 2009, pp. 1378-1383, doi: 10.1109/PEDS.2009.5385741.

**Jialin Zheng** (S’19) received the B.S. degree in electrical engineering in 2019 from Beijing Jiaotong University,Beijing, China. Since 2019, he has been working toward the Ph.D. degree at the Department of Electrical Engineering, Tsinghua University, Beijing, China.

His research interests include simulation of power electronic systems, modeling of power semiconductor devices, and modeling for high capacity power electronics devices.

**Zhengming Zhao** (M’02–SM’03–F’18) received the B.S. and M.S. degrees in electrical engineering from Hunan University, Changsha, China, in 1982 and 1985, respectively, and the Ph.D. degree from Tsinghua University, Beijing, China, in 1991. From 1994 to 1996, he was a Postdoctoral Fellow with Ohio State University, Columbus, OH, USA, and then was a Visiting Scholar with the University of California, Irvine, CA, USA, for one year. He is currently a Professor with the Department of Electrical Engineering, Tsinghua University.

His research interests include high-power conversion, power electronics and motor control, and solar energy applications.

**Bochen Shi** (S’17) was born in Dalian, China, in 1995. He received the B.S. degree from the Departmentof Electrical Engineering, Tsinghua University, Beijing, China, in 2017, where he is currently working toward the Ph.D. degree in electrical engineering.

His research interests include modeling of power semiconductor devices, simulation framework of power electronic systems, and control strategies of power converters.

**Zhujun Yu** received the B.S. degree in 2018 from the Department of Electrical Engineering, Tsinghua University, Beijing, China, where she is currently working toward the Ph.D. degree in electrical engineering.

Her research interests include computer-aided simulation of power electronic systems and control strategies of power converters.

**Jiahe Ju** received the B.S. degree in 2018 from the Department of Electrical Engineering, Tsinghua University, Beijing, China, where she is currently working toward the M.S. degree in electrical engineering.

Her research interests include simulation framework of power electronic systems and control strategies of power converters.

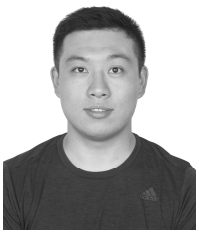

**Zhiqiang Fan** received the B.S. degree in electrical engineering in 2018 from the College of electrical and power engineering, Taiyuan University of Technology, Shanxi, China.

He is currently working toward the M.S. degree in electrical engineering in the Department of Electrical Engineering, Tsinghua University, Beijing, China.